Modeling of the light transfer in a water column polluted with oil suspension

Z. A. Otremba
zotremba@am.gdynia.pl
Gdynia Maritime University, Physics Department, Gdynia, 81225, Poland

The radiance field in oil-polluted seawater determined at various depths for the central band of the light spectrum (547 nm) is considered. In the aquatic model, a flat sea surface, a cloud-free sky and selected inherent optical properties (IOPs) of natural seawater and oil-in-water emulsion are taken into account. The representative results of Monte Carlo photon trace simulations are presented for the directional radiance distribution (L), the directional distribution of the radiance reflectance (R_L) and the intensity of downward and upward irradiance (E). [DOI: http://dx.doi.org/10.2971/jeos.2013.13067]

Keywords: Radiative transfer, seawater, oil suspension, photon trace simulation, environmental monitoring

1 INTRODUCTION

Oil residuals are among the many factors influencing the radiance distribution in the seawater column. The appearance of oil in the sea is caused by both natural phenomena (mainly oil seeps [1]) and human activities (discharges of sewage from ships, naval accidents, land inflow [2]). Knowledge of the dependence of spatial, directional and spectral distribution of the radiance in the future will be useful for estimating how oil disturbs optical observations of natural processes in the euphotic zone of the sea and the concentration and extension of oil migration in the marine environment in its surface (oil film, water-in-oil emulsion) or underwater form (oil-in-water emulsion). The manifestation of the presence of oil depends not only on the optical properties of oil, but also on the optical properties of the natural components of the seawater. Since it is impossible to formulate universal rules on how oil substances control radiance distribution [3], the configurations of optical properties of natural water components and the optical properties of various oils (which result in significant changes in the radiance field) are worth studying.

Spectra of both absorption and scattering coefficients and the volume scattering functions for various wavelengths, as well as their spatial distribution, are required to derive directional radiance distribution in the water column. On the other hand, directional radiance distribution can serve as the source data to derive quantities which are currently in use in operational oceanography, i.e. the radiance reflectance R_L (including R_L for vertical direction, called Remotely Sensed Reflectance - RSR) or the irradiance reflectance R_E.

Consequences of the presence of the alien substances (oil emulsion example) in the seawater for above-water R_L (named Remote Sensing Reflectance R_{sr}) has been already shown [3], although this paper presents the spatial and directional distribution of the radiance in a seawater column polluted with oil emulsion (1 ppm) in comparison to a non-polluted one. A photon Monte Carlo trace simulation was used in the modeling underwater radiance field while assuming water optical properties typical of the environment as well as the previously determined optical properties of the oil emulsion. In relation to possible measurements in the real environment, the results presented here should be treated as time-averaged ones, whereas an approach suitable for measuring the instantaneous values of optical properties was reported by Hieronymi [4].

2 METHOD

In this study, the model of the seawater body consists of the exemplary inherent optical properties (IOPs) for natural (free of oil) seawater and for the same seawater, but polluted with oil-in-water emulsion. Additionally, the model assumes that the surface of the sea is flat, the zenithal position of the sun is 30° and the part of photons diffused in the free of clouds sky is 20 %.

The optical features of natural waters have been studied for many years. Since the 1970s there have been many attempts to optically classify the marine waters through their color [5] in relation to their turbidity [6]. Currently, we know that marine waters are highly diversified in terms of IOPs. The direct measurement of the set of IOPs in the sea is not easy (no devices for automatic *in situ* measurements). If the VSF (Volume Scattering Function) measurements are considered, only fragments of VSF are measured directly in the sea (for a limited range of scattering angles) [7].

Determination of IOPs for oil-in-water emulsion is possible thanks to the so-called "Mie solution" [8] in which oil droplets are considered as homogenous spheres of various diameters described by size distribution. In addition to oil droplet size distribution, the input data for IOPs calculations include the spectra of absorption coefficient and the spectra of refraction

Received April 30, 2013; resubmitted August 22, 2013; accepted September 08, 2013; published October 03, 2013 ISSN 1990-2573

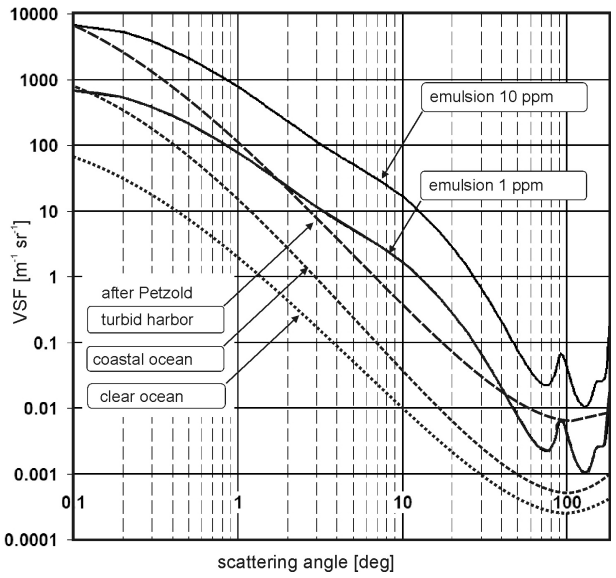

FIG. 1 Difference between volume scattering functions (VSFs) for oil-in-water emulsion and for natural water reported by Petzold [3]. In this study, VSFs in simulations for the emulsion of 1 ppm and for "clear ocean" water free of oil were used.

coefficient of oil. The output data in the Mie solution are the spectra of absorption coefficient "a" and the scattering coefficient "b" as well as VSF.

Angular distributions of the radiance at various depths were modeled by the Monte Carlo simulation. Underwater (virtual) radiance detectors were placed in 3,672 directions (1,836 for the upper hemisphere and the same number for the lower one). Every run of the Monte Carlo simulation consisted of 2 billion virtual photons.

Figures 1–3 present the IOP values, used further in the Monte Carlo simulations compared to all the values typical of the environment. Figure 1 presents components of IOPs which are exemplary VSFs of natural seawater and artificial water polluted with an oil-in-water emulsion, both in the same coordinate system. Three optically different kinds of natural sea water are represented by the plots according to Petzold [9]. Oiled water is represented by two plots – for crude oil *Romashkino* dispersed in seawater in concentrations 1 and 10 ppm. The large difference in VSF shapes for natural seawater and water polluted with oil suggest that the spatial peregrinations of photons in those two kinds of water should be different (which is reflected in the spatial and directional distribution of the radiance). The optical properties of seawater are still uncertain – the latest data was reported by Freda and Piskozub [7] using the diversity of shapes of VSFs in terms of light leaving the sea surface.

3 RESULTS

Every run of the Monte Carlo simulator resulted in an output file which contains numerical tables of values proportional to radiances for 3,672 directions of the whole sphere in various depths. These values are the basis for determining various optical values: radiance coefficient $L'(\theta,\phi)$ at depth z is calculated from formula (1), radiance reflectance - from (2), radiance transmittance - from (3).

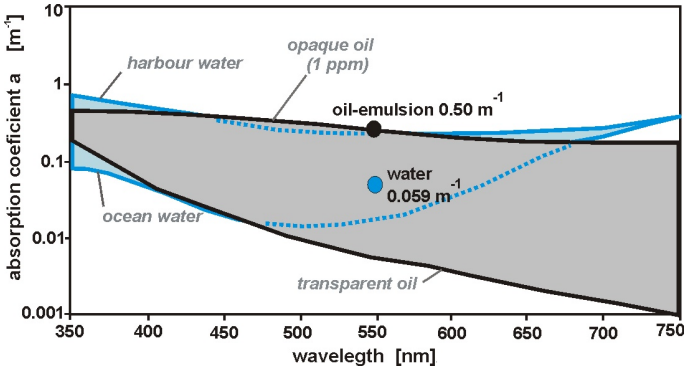

FIG. 2 Spectra of absorption coefficient (blue zone) for natural seawater and for oil emulsions of 1 ppm (grey zone). The black dot represents the absorption coefficient for oil suspension, whereas the blue dot represents water free of oil (both applied in this study).

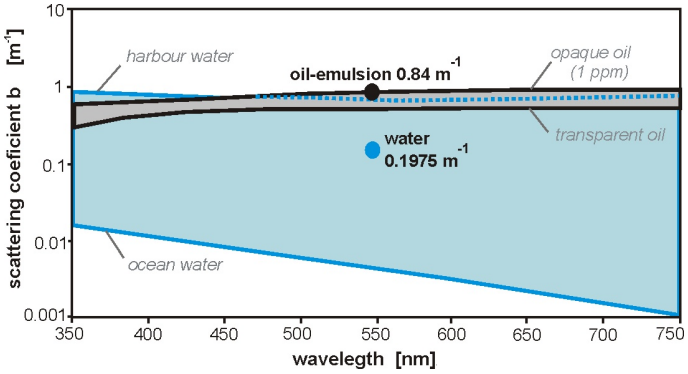

FIG. 3 Spectra of scattering coefficient (blue zone) for natural seawater and for oil emulsions of 1 ppm (grey zone). The black dot represents the scattering coefficient for emulsion, whereas the blue dot represents water free of oil (both applied in this study).

$$L'(z,\theta,\varphi) = \frac{L(z,\theta,\varphi)}{E_d(z=0^-)} \tag{1}$$

where:

θ-zenith angle
ϕ-azimuth angle
$L(z,\theta,\phi)$-radiance distribution for the whole sphere at depth z
$E_d(z=0^-)$-downward irradiance just above the sea surface

Radiance coefficient is a value which corresponds to a possible practical situation when the radiance angular distribution is measured in the water column, whereas downward irradiance is just above the sea surface.

Radiance reflectance R_L and radiance transmittance T_L is when both radiance angular distribution and downward irradiance are measured in the water column.

$$R_L(z,\theta,\varphi) = \frac{L_u(z,\theta,\varphi)}{E_d(z)} \tag{2}$$

where:

$L_u(z,\theta,\phi)$-upward radiance distribution for the upper hemi-

sphere at depth z
$E_d(z)$-downward irradiance at depth z

$$T_L(z,\theta,\varphi) = \frac{L_d(z,\theta,\varphi)}{E_d(z)} \tag{3}$$

where:

$L_d(z,\theta,\phi)$-downward radiance distribution for the upper hemisphere on depth z
$E_d(z)$-downward irradiance at the depth z

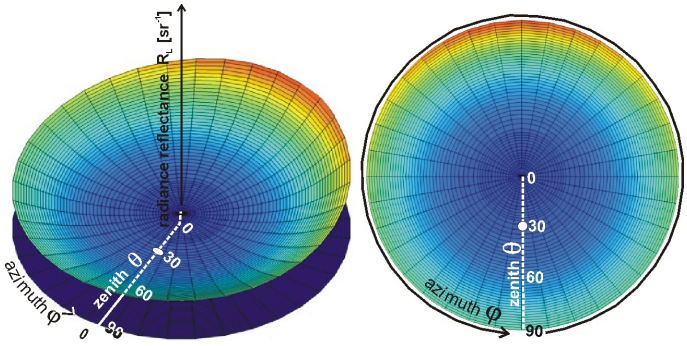

FIG. 4 Principle of visualization applied in this paper for directional underwater distribution of radiance coefficient, radiance reflectance and radiance transmittance. The white dot represents the directional position of the sun (30^o). The above example case is extracted from Figure 6 (radiance reflectance, free of oil, 1 m).

Cylindrical coordinates as 3D graphs are used in order to illustrate the results obtained (explained in Figure 4). The white dot in Figure 4 represents the directional position of the sun in every case described further in this paper. Every visualization of spatial distribution is shown twice: on the left on the color scale plus the 3D shape, whereas on the right it is shown only on the color scale. Selected visualizations have cut out high values (grey area) to achieve better graphical clarity.

The angular distribution of the radiance illustrates the radiance coefficient represented by Figure 5. The same data as those used for the results represented in Figure 5 are used to calculate radiance reflectance directional distribution R_L (2) and radiance transmittance distribution T_L (3). Figure 6 contains the angular distributions of those two values.

Figures 7 and 8 present diagrams using the same data as the ones used in Figures 5 and 6. The difference is that Figures 5 and 6 visualize numerical tables containing data for each azimuth angle, whereas Figures 7 and 8 are based on data extracted from those tables for only the direction in the plane of the solar light.

4 DISCUSSION

The presented information on optical processes in the seawater column has an exemplary nature and represents se-

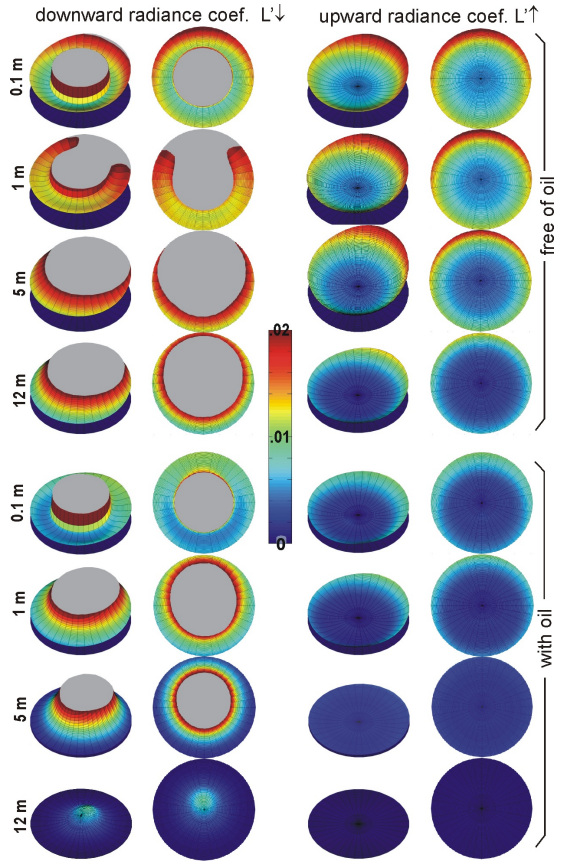

FIG. 5 Shapes of directional distribution of the radiance coefficient in a water column free of oil (upper graphs) and polluted with oil (lower graphs). The grey area indicates the level above which the values are hidden. The position of the sun in Figure 4 is shown.

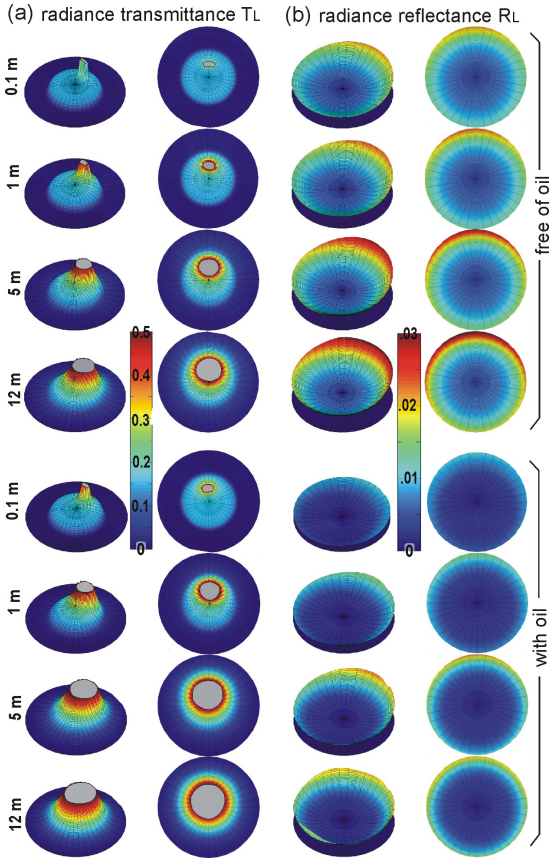

FIG. 6 Shapes of directional distribution of the radiance transmittance in a water column free of oil (upper left graphs) and polluted with oil (lower left graphs) (a) and directional distribution of the radiance reflectance in a water column free of oil (upper right graphs) and polluted with oil (lower right graphs) (b).

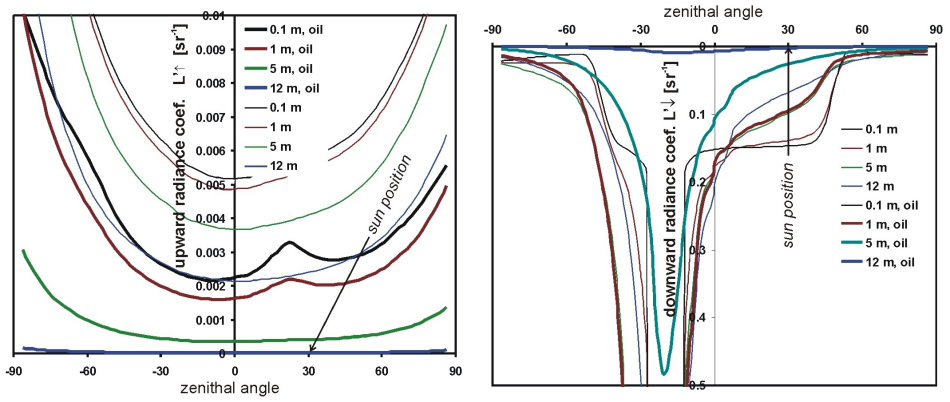

FIG. 7 Radiance coefficient as a function of zenithal angle (from -90^0 to +90^0) in the plane of solar light for upward direction (left) and for downward direction (right). Graphs prepared on the basis of the same data as in Figure 5.

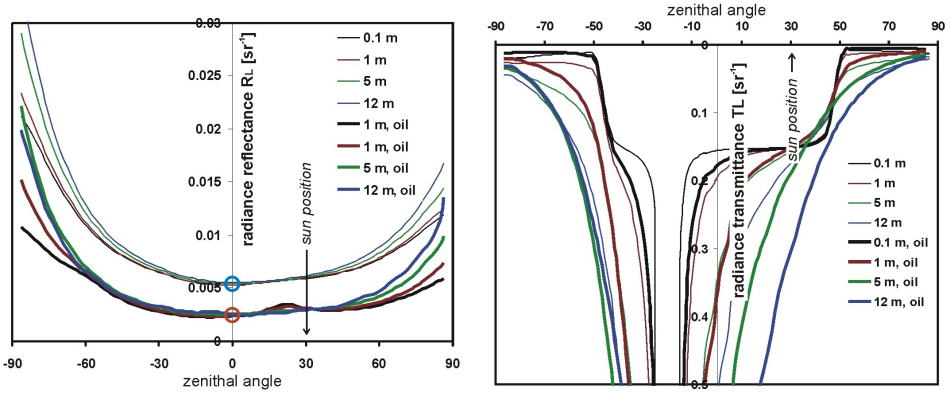

FIG. 8 Radiance reflectance (left) and radiance transmittance (right) as a function of zenithal angle (from -90^0 to +90^0) in the plane of solar light. The graphs were prepared on the basis of the same data as in Figure 6. Blue and brown circles in the upper graph show reflectance observed perpendicularly (Remote Sensed Reflectance RSR).

lected scenarios which are likely to occur in the environment. Their current function is to improve the understanding of interactions between light and seawater constituents, especially when the sea area is polluted by incidentally occurring substances, environmentally alien (in this case, oil emulsion). The presentation of a larger amount of information requires extended study, taking into account the data not only used in the present study (absorption coefficient and scattering coefficient represented by the black and yellow dots in Figures 2 and 3) but also various combinations of the data from the signed area in the same picture. An open problem remains the shape of the volume scattering function (VSF) in various regions of the sea in various seasons and for defined phases of annual biological processes.

The principal finding from the above data is that oil suspended in the seawater even in small concentrations (i.e. 1 ppm) significantly modifies the underwater light field. This modification manifests itself by changing the shape of angular distributions of radiance reflectance $R_L(z,\theta,\phi)$ and radiance transmittance $R_T(z,\theta,\phi)$ as well as radiance $L(z,\theta,\phi)$ represented by the radiance ratio $L'(z,\theta,\phi)$ (which is proportional to the radiance). The radiance ratio is a useful value for the actual radiance $L(z,\theta,\phi)$ calculation when the above-sea-surface irradiance $E(z=0^-)$ is known (see formula (1)). On the other hand, both radiance reflectance $R_L(z,\theta,\phi)$ and radiance transmittance $R_T(z,\theta,\phi)$ are used for calculating the angular distribution of the radiance $L(z,\theta,\phi)$ for the whole sphere when downward irradiance in a defined depth can be known (see formulas (2) and (3)). In addition, the angular distribution of the radiance allows data on the water constituents to be assessed (through their input into IOPs). To better illustrate this problem, a comparison of sample distributions of the normalized radiance $(L(z,\theta,\phi)/L_{max})$ for water free of oil and water polluted with oil for the same environmental scenarios in Figure 9 is shown.

In addition, besides the changes in the radiance distribution, changes in the absolute values of radiances also occur. For example, this is illustrated by comparing two analogical graphs in Figure 9 (where the radiance is normalized to the maximum) and Figure 5 (no normalization) – namely, column three and row seven (depth 5 m): it is seen that oil suspension results in the radiance decreasing in every direction. It is also demonstrated in Figure 10, in which both irradiances: downward (due to definition 4) and upward (def. 5) on various depths are shown.

$$E_d(z) = \int_0^{2\pi} \int_0^{\pi/2} L(z,\theta,\varphi)\ \cos\theta \sin\theta\ d\theta\ d\varphi \tag{4}$$

$$E_u(z) = \int_0^{2\pi} \int_{\pi/2}^{\pi} L(z,\theta,\varphi)\ \cos\theta \sin\theta\ d\theta\ d\varphi \tag{5}$$

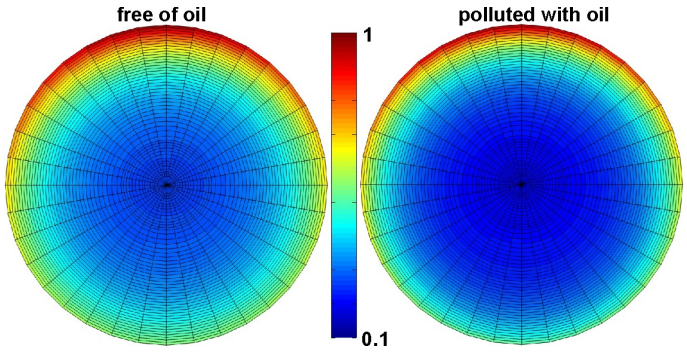

FIG. 9 Comparison of angular distribution of normalized radiance $(L(\theta,\phi)/L_{max})$ for clear and oiled seawater (prepared from the same data set as in Figs. 5 and 6, depth 5 m).

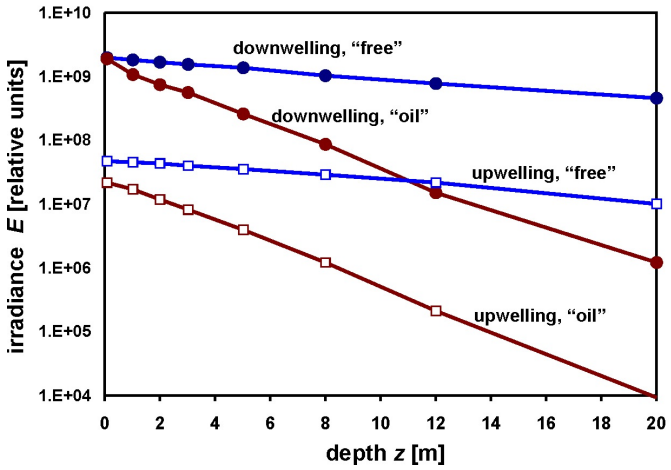

FIG. 10 Comparison of upwelling and downwelling irradiance for a water column free of oil ("free") and polluted by an oil-suspension ("oil").

The data shown in Figure 10 were used to prepare Figure 11, in which irradiance reflectance $R_E(z)$ (due to definition (6)) for both water columns (free of oil and polluted with oil) is shown. Irradiance reflectance in water free of oil increases in the analyzed range of depth (0 – 30 m), whereas the level of irradiance in water polluted with oil stabilizes at 10 m. Obviously, the plot of the relationship between the irradiance and the depth will depend on the concentration of oil.

$$R_E(z) = \frac{E_u(z)}{E_d(z)} \tag{6}$$

where:

$E_u(z)$-upward irradiance on the depth z
$E_d(z)$-downward irradiance on the depth z

The information presented in this study applies only to one wavelength (547 nm, the central band of the visible light spectrum) and to one combination of IOPs indicated in Figures 1–3. The next step towards improving an understanding of the modification of the optical properties in the sea polluted with oil emulsion would be to analyze every above-mentioned quantity in various wavelengths and for various geometrical and weather scenarios and various IOPs,

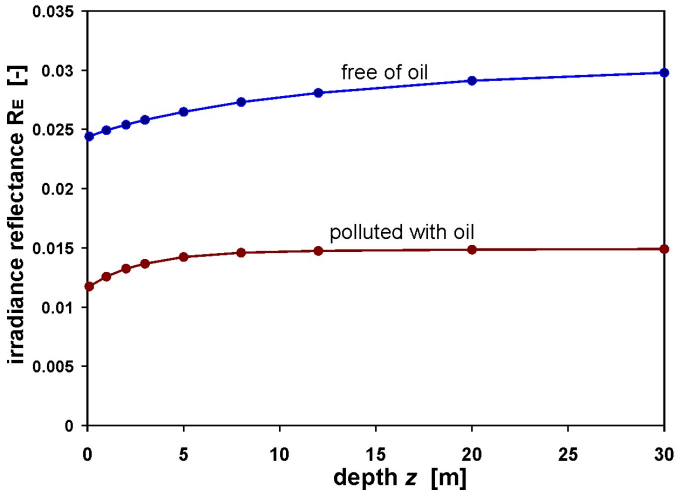

FIG. 11 Irradiance reflectance vs. depth for free of oil and for a water column polluted with oil.

depending on the sea region or current optical condition at a defined point of the sea.

Currently, characterizing the aquatic environment by the angular distribution of radiance is not so popular because of the widespread spectral analyses performed using both RSR and R_E meters. However, angular analyses have been a subject of interest since the 1950s [10]. The rapid development of techniques for *in situ* measurement of the angular distribution of the radiance [11] forms a solid foundation for the completion of spectral methods with directional methods.

5 ACKNOWLEDGEMENTS

This work was supported by Gdynia Maritime University grant No. DS360.

References

[1] *Oil in the Sea III: Inputs, Fates, and Effects* (The National Academies Press, Washington, 2003).

[2] M. Fingas, *Oil Spill Science and Technology* (Elsevier, Amsterdam, 2011).

[3] Z. Otremba, "Optical contrast of oil dispersed in seawater under windy conditions," J. Europ. Opt. Soc. Rap. Public. **8**, 13051 (2013).

[4] M. Hieronymi, "Monte Carlo code for the study of the dynamic light field at the wavy atmosphere-ocean interface," J. Europ. Opt. Soc. Rap. Public. **8**, 13039 2013.

[5] A. Morel, and L. Prieur, "Analysis of variations in ocean color," Limnology and Oceanography **22(4)**, 709–722 (1977).

[6] C. D. Mobley, D. Stramski, W. P. Bissett, and E. Boss, "Optical Modeling of Ocean Water - Is the Case 1 - Case 2 Classification Still Useful?," Oceanography **17(2)**, 60–67 (2004).

[7] W. Freda, and J. Piskozub, "Revisiting the role of oceanic phase function in remote sensing reflectance," Oceanologia **54**, 29–38 (2012).

[8] C. F. Bohren, and D. R. Huffmann, *Absorption and scattering of light by small particles* (Willey, New York, 1983).

[9] T. J. Petzold, "Volume scattering functions for selected ocean waters," in *Light in the Sea*, J. E. Tyler, ed. (Hutchinson & Ross, Dowden, 1977).

[10] J. E. Tyler, "Radiance distribution as a function of depth in an underwater environment," Bulletin of the Scripps Institute of Oceanography **7**, 363–411 (1960).

[11] D. Antoine, A. Morel, E. Leymarie, A. Houyou, B. Gentili, S. Victori, J.P. Buis, et al., "Underwater Radiance Distributions Measured with Miniaturized Multispectral Radiance Cameras," Journal of Atmospheric and Oceanic Technology **30**, 74–95 (2003).